4892 *Chem. Mater.* **2009,** *21,* 4892–4898
DOI:10.1021/cm902667b

CHEMISTRY OF MATERIALS
Article

A Facile Approach to Fabrication of Bifunctional Magnetic-Optical Fe_3O_4@ZnS Microspheres

Xuegang Yu,[†] Jiaqi Wan,[†] Yan Shan,[†] Kezheng Chen,*[,†] and Xiaodong Han[‡]

[†]*College of Materials Science and Engineering, Qingdao University of Science and Technology, Qingdao 266042, China, and* [‡]*Institute of Microstructure and Property of Advanced Materials, Beijing University of Technology, Beijing 100124, China*

Received July 3, 2009

Bifunctional magnetic-optical Fe_3O_4@ZnS microspheres with core−shell heterostructures have been successfully fabricated by a simple chemical deposition method. The adsorption of sodium dodecyl sulfate (SDS) on the preformed magnetite microspheres played an essential role in directing the structure of the composites. The presented materials were characterized by FE-SEM, HRTEM, XRD, FTIR, fluorescence spectrophotometer, and SQUID MPMS. The results showed that spherical Fe_3O_4 cores were coated by a uniform ZnS layer. The saturation magnetization value of Fe_3O_4@ZnS core−shell microspheres is 52.5 emu g^{-1} at room temperature. Ultraviolet and visible light can be easily obtained by exposing the microspheres to different excitation wavelengths. The combined magnetic and fluorescent properties endow the microspheres with great potential applications in drug targeting, bioseparation and diagnostic analysis.

1. Introduction

Recently, there has been growing research interest in magnetic-optical materials with core−shell heterostructures because of the integrated functionalities of cores and shells.[1−4] The combined magnetic-optical properties endow the composites with a promising application in biomedical fields including drug targeting, bioseparation, and diagnostic analysis.[5−7] Among magnetic materials, iron oxide (γ-Fe_2O_3 or Fe_3O_4) is superior to others because of their special magnetic properties and low toxicity.[8−12] The magnetic iron oxide has shown great applications in ferrofluids,[13] magnetic storage media,[14] stem cell labling,[15] magnetic resonance imaging (MRI).[16−18]

High-photostability fluorescent materials are attracting increasing attention in biological fields.[19−21] Yu et al. used lanthanide ions (Tb^{3+}) to prepare Fe_3O_4@SiO_2@-PABI-Tb magnetic-optical nanoparticles.[22] Yoon et al. succeed in achieving specific targeting, cell sorting, and bio-imaging by using organic dye (fluorescein isothiocyanate, FITC).[23] Kim et al. used FITC and rhodamine B isothiocyanate (RITC) to prepare Fe_3O_4@SiO_2 nanoparticles, which provided a practical application in MR, fluorescence imaging and drug delivery.[24] However, lanthanide ions and organic dye can't be used widely because of their high radioactivity and expensive price. It's well known that zinc sulfide (ZnS) has the largest energy band gap among the II−VI compound semiconductors of direct transition type,[25] and can be used for the

*To whom correspondence should be addressed. Tel: +86-532-84022509. Fax: +86-532-84022509. E-Mail: kchen@qust.edu.cn.

(1) Gao, J.; Zhang, B.; Gao, Y.; Pan, Y.; Zhang, X.; Xu, B. *J. Am. Chem. Soc.* **2007**, *129*, 11928.
(2) Bao, Y.; Calderon, H.; Krishnan, K. M. *J. Phys. Chem. C* **2007**, *111*, 1941.
(3) Salgueiriño-Maceira, V.; Correa-Duarte, M. A.; Spasova, M.; Liz-Marzán, L. M.; Farle, M. *Adv. Funct. Mater.* **2006**, *16*, 509.
(4) Hu, S.-H.; Chen, S.-Y.; Liu, D.-M.; Hsiao, C.-S. *Adv. Mater.* **2008**, *20*, 2690.
(5) Lee, I. S.; Lee, N.; Park, J.; Kim, B. H.; Yi, Y.-W.; Kim, T.; Kim, T. K.; Lee, I. H.; Paik, S. R.; Hyeon, T. *J. Am. Chem. Soc.* **2006**, *128*, 10658.
(6) Tang, D.; Yuan, R.; Chai, Y.; An, H. *Adv. Funct. Mater.* **2007**, *17*, 976.
(7) Park, H.-Y.; Schadt, M. J.; Wang, L.-Y.; Lim, I.-I. S.; Njoki, P. N.; Kim, S. H.; Jang, M.-Y.; Luo, J.; Zhong, C.-J. *Langmuir* **2007**, *23*, 9050.
(8) Deng, Y.; Qi, D.; Deng, C.; Zhang, X.; Zhao, D. *J Am. Chem. Soc.* **2008**, *130*, 28.
(9) Xu, X.; Deng, C.; Gao, M.; Yu, W.; Yang, P.; Zhang, X. *Adv. Mater.* **2006**, *18*, 3289.
(10) Park, J.; An, K.; Hwang, Y.; Park, J.-g.; Noh, H.-j.; Kim, J.-y.; Park, J.-h.; Hwang, N.-m.; Hyeon, T. *Nat. Mater.* **2004**, *3*, 891.
(11) Mori, K.; Kondo, Y.; Morimoto, S.; Yamashita, H. *J. Phys. Chem. C* **2008**, *112*, 397.
(12) Zhu, A.; Yuan, L.; Dai, S. *J. Phys. Chem. C* **2008**, *112*, 5432.
(13) Sun, S.; Zeng, H. *J. Am. Chem. Soc.* **2002**, *124*, 8204.
(14) Sun, S.; Murray, C. B.; Weller, D.; Folks, L.; Moser, A. *Science* **2000**, *287*, 1989.
(15) Babič, M.; Horák, D.; Trchová, M.; Jendelová, P.; Glogarová, K.; Lesný, P.; Herynek, V.; Hájek, M.; Syková, E. *Bioconjugate Chem.* **2008**, *19*, 740.
(16) Wan, J.; Cai, W.; Meng, X.; Liu, E. *Chem. Commun.* **2007**, 5004.
(17) Hultman, K. L.; Raffo, A. J.; Grzenda, A. L.; Harris, P. E.; Brown, T. R.; O'Brien, S. *ACS Nano* **2008**, *2*, 477.
(18) Shi, X.; Wang, S. H.; Swanson, S. D.; Ge, S.; Cao, Z.; Antwerp, M. E. V.; Landmark, K. J.; , J. R. B.Jr. *Adv. Mater.* **2008**, *20*, 1671.
(19) Lo, K. K.-W.; Louie, M.-W.; Sze, K.-S.; Lau, J. S.-Y. *Inorg. Chem.* **2008**, *47*, 602.
(20) Wilhelm, C.; Lavialle, F.; Péchoux, C.; Tatischeff, I.; Gazeau, F. *Small* **2008**, *4*, 577.
(21) Louis, C.; Bazzi, R.; Marquette, C. A.; Bridot, J.-L.; Roux, S.; Ledoux, G.; Mercier, B.; Blum, L.; Perriat, P.; Tillement, O. *Chem. Mater.* **2005**, *17*, 1673.
(22) Yu, S.-Y.; Zhang, H.-J.; Yu, J.-B.; Wang, C.; Sun, L.-N.; Shi, W.-D. *Langmuir* **2007**, *23*, 7836.
(23) Yoon, T.-J.; Yu, K. N.; Kim, E.; Kim, J. S.; Kim, B. G.; Yun, S.-H.; Sohn, B.-H.; Cho, M.-H.; Lee, J.-K.; Park, S. B. *Small* **2006**, *2*, 209.
(24) Kim, J.; Kim, H. S.; Lee, N.; Kim, T.; Kim, H.; Yu, T.; Song, I. C.; Moon, W. K.; Hyeon, T. *Angew. Chem., Int. Ed.* **2008**, *47*, 8438.
(25) Zhao, L.; Gao, L. *J. Mater. Chem.* **2004**, *14*, 1001.

Published on Web 09/28/2009

fabrication of photonic crystals,[26] light-emitting diodes (LED),[27] solar cells,[28] and so on. Compared with other fluorescent materials, ZnS has great advantages as follows: (1) strong fluorescent property (2) environment-friendly, (3) relative lower price, (4) simple synthesis procedure. Therefore, ZnS is one suitable component to synthesize high-photostability fluorescent materials.

On the basis of the above discussion, bifunctional magnetic-optical Fe_3O_4@ZnS composites with core−shell structures show a great potential application in biological field. However, because of the lattice mismatch of the components, it's difficult for zinc sulfide to coat magnetic iron oxide directly. To solve the problem, some certain amorphous transition layers can be used in the synthesis of core−shell materials. For instance, Chen et al. synthesized well-defined core−shell Fe_3O_4@SiO_2@CdS spheres by using amorphous silica as the spacer.[29] Li et al. used the amorphous carbon layer as the spacer to synthesize Fe_3O_4@C@TiO_2 core−shell microspheres.[30] Although they prepared the corresponding materials, the synthetic procedure is rather complex and time-consuming.

In the present work, we designed a facile approach for fabricating bifunctional magnetic-optical Fe_3O_4@ZnS core−shell microspheres without using other components as a transition layer. The resulting microspheres possess the advantages of uniform sizes, robust magnetization, and strong fluorescence. Furthermore, the current facile synthetic procedure may be extended to the fabrication of other bi- or multifunctional composites by using different cation or anion surfactants.

2. Experimental Section

2.1. Materials. Analytical ferric chloride hexahydrate ($FeCl_3 \cdot 6H_2O$), sodium acetate (NaAc), sodium dodecyl sulfate (SDS), zinc acetate ($Zn(Ac)_2$), thioacetamide (TAA), and solvents were purchased from Shanghai Chemical Reagents Company. All chemicals were used without further purification. High purity water (18.2 MΩ cm) was obtained from a Milli-Q system (Millipore) and used in all the experiments.

2.2. Synthesis of Fe_3O_4 Microspheres. The magnetic particles were prepared by polyol media solvothermal method according to the method reported with minor modification.[31] Typically, 2.4 g (8.88 mmol) of $FeCl_3 \cdot 6H_2O$ was dissolved in 60 mL of ethylene glycol (EG) to form a stable orange solution. Then, 8 g (5.88 mmol) of NaAc was added into the above solution under vigorous magnetic stirring for 30 min until completely dissolved. The as-formed solution was transferred into a Teflon-lined stainless-steel autoclave of 100 mL capacity and sealed to heat at 200 °C for 8 h. After cooling to room temperature, the obtained black magnetite particles were washed with water and ethanol several times, and then dried in a vacuum at 60 °C for 12 h.

2.3. Fabrication of Fe_3O_4@ZnS Microspheres with Core−Shell Structures. In a typical procedure, 0.3 g (1.29 mmol) of Fe_3O_4 particles were treated with 100 mL 0.05 M HCl aqueous solution by ultrasonication.[8] After the treatment for 30 min, the Fe_3O_4 particles were washed with water for several times, and then redispersed into a SDS (0.2 g, 0.69 mmol) aqueous solution under vigorous stirring for 24 h. The treated magnetite particles were separated, and then dispersed in 60 mL of $Zn(Ac)_2$ (0.44 g, 2.4 mmol) isopropanol solution. The obtained mixture was stirring at room temperature for 24 h. After that, the mixture was transferred to a water bath and 60 mL of TAA (0.2 g, 2.66 mmol) aqueous solution was added dropwise. At the same time, the resulting solution was heated to 65 °C and kept at that temperature under vigorous stirring. After the reaction for 6 h, the product was magnetically collected and washed with water and ethanol for several times to remove the excess ZnS nanoparticles. The as-prepared sample was dried in a vacuum at 60°C for 12 h, and then kept in a desiccator for later characterization.

2.4. Characterization. FE-SEM images were collected on a field-emission scanning electron microscopy (JEOL JSM-6700F). The TEM observation was conducted using the JEOL 2010 TEM with operating voltage at 200 KV. The high-resolution electron microscopy (HRTEM) experiments were conducted using a field emission gun (FEG) JEOL 2010F microscope with a point resolution of 0.19 nm. EDS was recorded on an energy X-ray microanalysis system (JEOL B^5-U^{92}), which was attached to the JEOL 2010F electron microscope. Because the diameter of prepared Fe_3O_4@ZnS microsphere was relatively large, it is difficult for us to observe its core−shell structures directly using TEM and HRTEM. To solve this problem, were first dispersed the Fe_3O_4@ZnS microspheres in the polymer resin. And after the solidification of the polymer resin, the samples were cut into thin slices with about 120 nm thickness using ultramicrotome (PowerTomeXL). The XRD patterns were recorded on a powder X-ray diffractometer (Rigaku D/max-rA) equipped with a rotating anode and a Cu $K_{\alpha 1}$ radiation source (λ = 1.5406 Å) at a step width of 0.02°. The photoluminescence spectra of the samples were measured on a Hitachi F-4600 fluorescence spectrophotometer. A Nikon Eclipse TE2000-S inverted fluorescence microscope was used to visualize all fluorescent samples. Magnetic measurement of the products was conducted on Quantum Design SQUID MPMS-5XL magnetometer. Infrared spectra were obtained on a Bruker TENSOR27 FTIR spectrometer.

3. Results and Discussion

3.1. Structure and Morphology of Fe_3O_4 and Fe_3O_4@ZnS Microspheres. Figure 1 illustrates XRD patterns of as-synthesized Fe_3O_4 and Fe_3O_4@ZnS microspheres. In curve a, all the diffraction peaks can be indexed to face-centered cubic structure of magnetite according to JCPDS card NO. 19-0629. In curve b, besides the corresponding peaks of magnetite, all the others can be indexed to hexagonal wurtzite ZnS, which correspond to JCPDS card 12-0688 and the broad diffraction peaks indicate the small size of ZnS nanoparticles.

SEM and TEM were employed to examine the detailed structure and morphology of as-synthesized Fe_3O_4 and Fe_3O_4@ZnS microspheres. Figure 2 reveals their typical SEM and low-magnification TEM images. From Figure 2a, it can be seen that the Fe_3O_4 microspheres

(26) Hosein, I. D.; Liddell, C. M. *Langmuir* **2007**, *23*, 2892.
(27) Kim, M. R.; Kang, Y.-M.; Jang, D.-J. *J. Phys. Chem. C* **2007**, *111*, 18507.
(28) Issac, A.; Jin, S.; Lian, T. *J. Am. Chem. Soc.* **2008**, *130*, 11280.
(29) Chen, M.; Gao, L.; Yang, S.; Sun, J. *Chem. Commun.* **2007**, 1272.
(30) Li, Y.; Wu, J.; Qi, D.; Xu, X.; Deng, C.; Yang, P.; Zhang, X. *Chem. Commun.* **2008**, 564.
(31) Deng, H.; Li, X.; Peng, Q.; Wang, X.; Chen, J.; Li, Y. *Angew. Chem., Int. Ed.* **2005**, *44*, 2782.

are composed of many Fe_3O_4 nanocrystals, and the structure isn't very close compact (shown as the arrows), which can be proved by the TEM image (Figure 2c). After being coated by zinc sulfide, the small holes formed by the Fe_3O_4 nanocrystals on the surface are disappeared, and the diameter of the spheres increased (Figure 2b). Figure 2d shows the obvious difference in contrast between the central part and the fringe, which indicates the ZnS layer had successfully deposited on the magnetite cores. The fragments around Fe_3O_4@ZnS microspheres in Figure 2d were produced by the ultramicrotome cutting. From Figure 2 and Table S1 (see the Supporting Information), it can be found the average diameters of the typical Fe_3O_4 and Fe_3O_4@ZnS microspheres are ~450.69 nm and ~518.81 nm, respectively. The thickness of ZnS layer is ~34.06 nm. When adding the different amounts of the $Zn(Ac)_2$ and TAA, the Fe_3O_4@ZnS microspheres with different thickness of ZnS layer can be obtained. The results are shown in Figure S2−S3 and Table S1 (see the Supporting Information). With increasing the concentrations of $Zn(Ac)_2$ and TAA, the thickness of ZnS layer is changed from 8.28 nm to 41.43 nm.

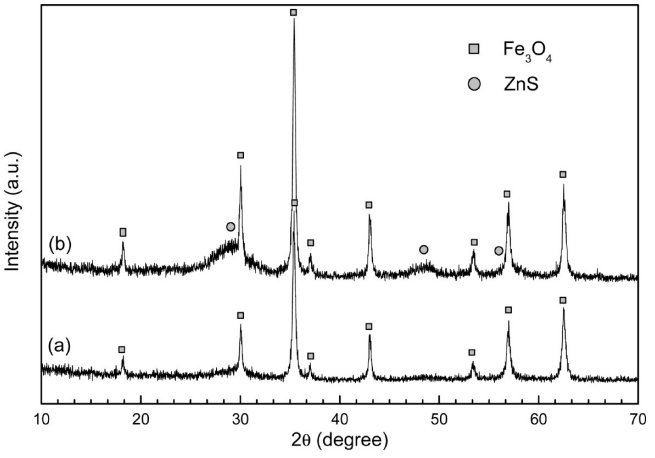

Figure 1. XRD patterns of (a) as-synthesized Fe_3O_4 microspheres and (b) Fe_3O_4@ZnS microspheres.

In order to further confirm the core−shell structure, high-magnification TEM and HRTEM characterizations were carried out (Figure 3). Figure 3a is a high-magnification bright field TEM image of a separated Fe_3O_4@ZnS microsphere, and it clearly shows the core−shell structures of Fe_3O_4@ZnS microsphere. The corresponding selected-area electron diffraction pattern (SAED) is shown in Figure 3b, which exhibits relative sharp diffraction spots, implying long-range ordering of the nanocrystals in the sample. Figure 3c shows the dark-field image from the selected $(\overline{1}11)$ reflection. The bright region illustrates the existence of the crystal grains whose oriented crystal plane meets the Bragg equation. HRTEM image of a selected area in Figure 3a is shown in Figure 3d, which provide more detailed structural information of the microspheres. The interlayer distances of Fe_3O_4 cores and ZnS shell are calculated to be ~0.26 nm and ~0.30 nm respectively, which agree well with the separation between the (331) lattice planes of face-centered cubic structure of magnetite and the (104) lattice planes of hexagonal wurtzite zinc sulfide. Images e and f in Figure 3 are the corresponding fast Fourier transform (FFT) images of the selected area of Figure 3d, which reveal the single-crystalline nature of the Fe_3O_4 core[31]

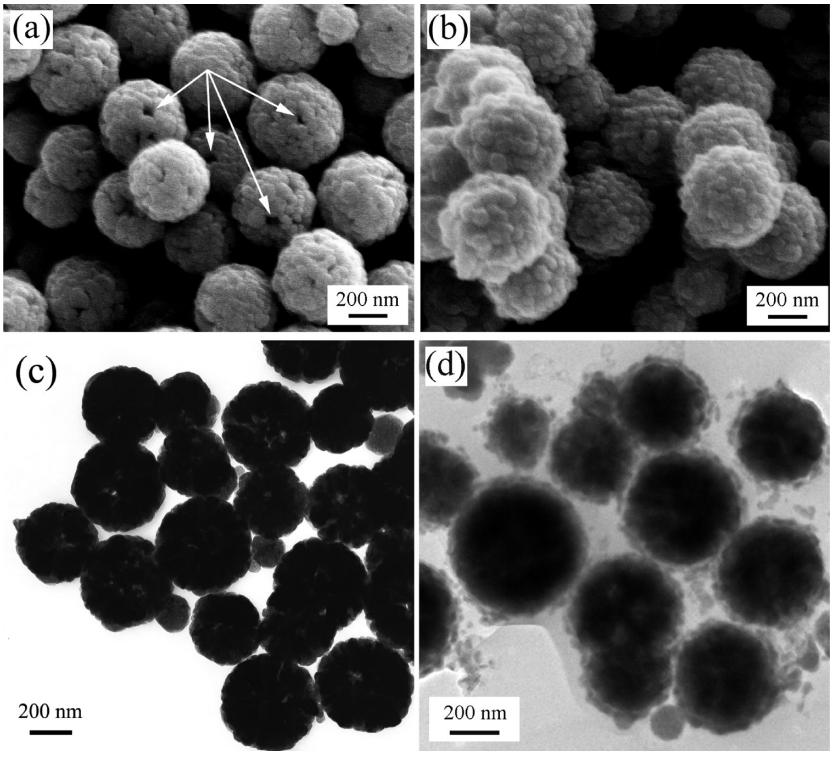

Figure 2. SEM images of (a) as-synthesized Fe_3O_4 microspheres and (b) Fe_3O_4@ZnS microspheres and low-magnification TEM images of (c) Fe_3O_4 microspheres and (d) the thin slices of Fe_3O_4@ZnS microspheres prepared by using ultramicrotome technique.

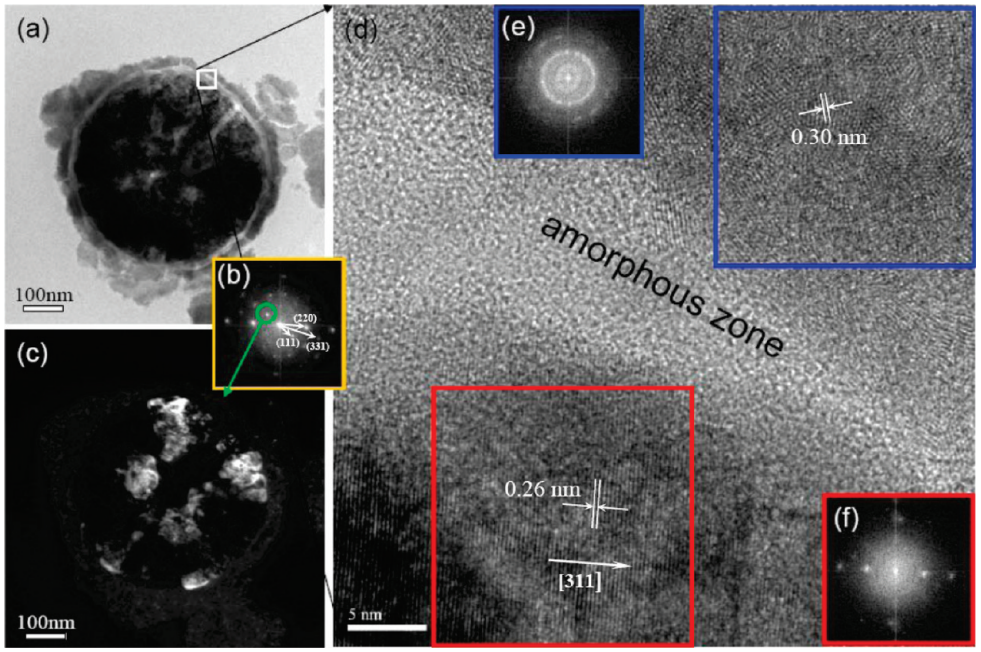

Figure 3. (a) High-magnification bright-field TEM image of thin slice of Fe_3O_4@ZnS microspheres prepared by using ultramicrotome technique. (b) selected-area electron diffraction pattern on a separated Fe_3O_4@ZnS microsphere. (c) Dark-field image of Fe_3O_4@ZnS microsphere, which obtained from the diffraction spot in the green circle. (d) HRTEM image of the selected area of (a). (e, f) Corresponding fast Fourier transform (FFT) images of the selected area of (d).

and multicrystalline nature of the ZnS shell. Further more, From the HRTEM image (Figure 3d), one can find that there is an amorphous layer between the crystallized Fe_3O_4 cores and ZnS layer. To explore the components and the formation mechanism of the amorphous layer, EDS analysis was carried out. Figure 4a is a bright-field TEM image of a separated Fe_3O_4@ZnS microsphere. The corresponding EDS elemental mappings are shown in Figure 4b−e, which illustrate the actual distribution of Fe, O, Zn, and S, separately. The core−shell structure can be easily observed. The EDS pattern Fe_3O_4@ZnS microsphere is shown in Figure 4f. There are no other elements existing in addition to the elements of Fe, O, Zn, and S in the samples. Furthermore, from Figure 4b−e and Figure S1 (see the Supporting Information), it can be found that the elemental location layer mainly corresponds to the location of Zn and S. On the basis of these results, we concluded that the interlayer is an amorphous layer of ZnS. The formation reason of the amorphous ZnS layer is related to the lattice matching. Because of the lattice mismatch of the components, it's difficult for crystallized zinc sulfide to coat crystallized magnetic iron oxide directly.[29,32] Therefore, in the reaction, amorphous ZnS was firstly generated as a transition layer on the surface of Fe_3O_4 core, which occurs at a relatively low reaction temperature at the beginning of the experiment.[32] The surface characteristics of Fe_3O_4 core were changed by amorphous ZnS layer, which would contribute to the deposition of the ZnS nanocrystals.

3.2. Optical and Magnetic Properties of Fe_3O_4@ZnS Microspheres. The photoluminescence (PL) spectra of Fe_3O_4@ZnS microspheres are presented in Figure 5. Figure 5a shows the main emission peak at 332 nm (3.74 eV, ultraviolet light) when excited by 225 nm Xe light, which corresponds to the intrinsic band-gap emission of bulk wurtize ZnS (3.7 eV).[33] In addition to the ultraviolet light, Figure 5b shows the as-synthesized composites also have a broad emission band 440−490 nm (blue light) when excited by 370 nm Xe light. The blue emission is tentatively attributed to the donor−acceptor pair transition in which the acceptor is related to the Zn^{2+} vacancy.[34,35] Therefore, for the Fe_3O_4@ZnS core−shell microspheres, ultraviolet and visible light can be easily obtained by using different excitation wavelength. The fluorescence microscopy images of Fe_3O_4 and Fe_3O_4@ZnS microspheres are shown in Figure 6. It can be seen that there is no light emission of pure Fe_3O_4 under UV light irradiation (Figure 6a). After coated by ZnS layer, the strong blue light emissions can be observed (Figure 6b). The fluorescence intensity of Fe_3O_4@ZnS microspheres with different thickness of ZnS layer was investigated. The results show that the fluorescence intensity of Fe_3O_4@ZnS microspheres increases with increasing the thickness of the ZnS layer (see the Supporting Information, Figure S4).

The magnetic properties of as-synthesized Fe_3O_4 and Fe_3O_4@ZnS microspheres measured at the temperatures of 300 and 5 K are shown in Figure 7. The saturation magnetization (M_s) values of Fe_3O_4 are 85.7 emu g^{-1}

(32) Gu, H.; Zheng, R.; Zhang, X.; Xu, B. *J. Am. Chem. Soc.* **2004**, *126*, 5664.
(33) Lippens, P. E.; Lannoo, M. *Phys. Rev. B* **1989**, *39*, 10935.
(34) Murase, N.; Jagannathan, R.; Kanematsu, Y.; Watanabe, M.; Kurita, A.; Hirata, K.; Yazawa, T.; Kushida, T. *J. Phys. Chem. B* **1999**, *103*, 754.
(35) Hu, P.; Liu, Y.; Fu, L.; Cao, L.; Zhu, D. *J. Phys. Chem. B* **2004**, *108*, 936.

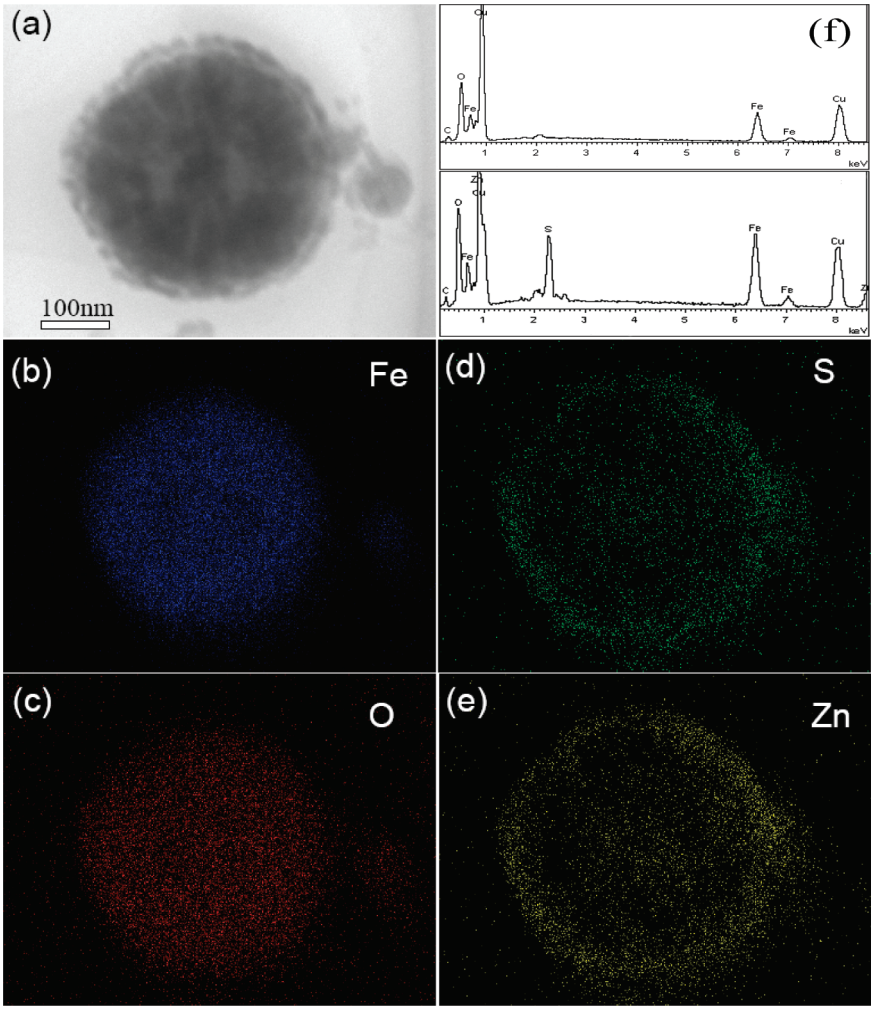

Figure 4. (a) High-magnification TEM image and (b−e) EDS elemental mappings of Fe_3O_4@ZnS microsphere. (f) EDS patterns of Fe_3O_4 and Fe_3O_4@ZnS microsphere.

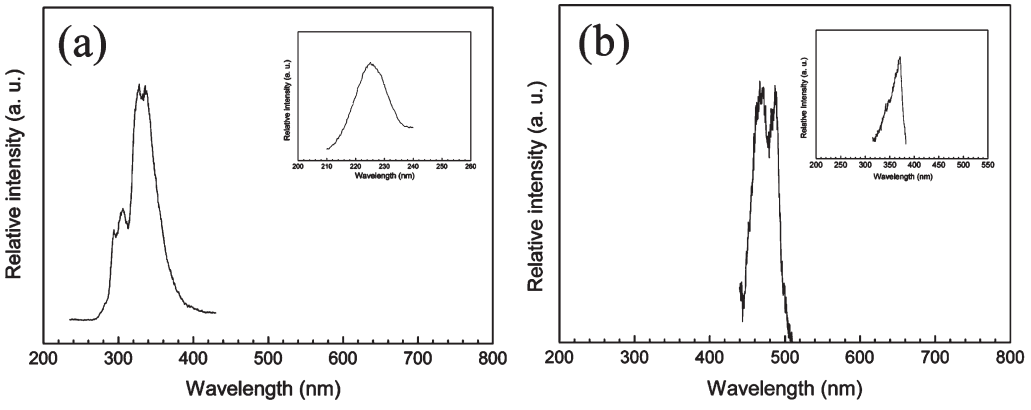

Figure 5. Room temperature photoluminescence emission spectra of Fe_3O_4@ZnS microspheres excited by (a) 225 and (b) 370 nm. The inset is the corresponding excitation spectra.

(at 300K) and 94.7 emu g^{-1} (at 5 K), which correspond to the values of magnetite reported.[36,37] After being coated by ZnS layer, the M_s values of the sample are 52.5 emu g^{-1} (at 300 K) and 58.1 emu g^{-1} (at 5 K), respectively. The decrease in magnetic saturation for Fe_3O_4@ZnS microspheres can be explained by taking into account the diamagnetic contribution of the thick ZnS layer surrounding the magnetic Fe_3O_4 cores.[3] From Figure 7a, the microspheres show fast movement to the applied field. It suggests that the microspheres possess excellent magnetic responsivity, which is an advantage to their applications. The magnified hysteresis loops (the insets in Figure 7) indicate the core−shell microspheres

(36) Zhao, L.; Zhang, H.; Xing, Y.; Song, S.; Yu, S.; Shi, W.; Guo, X.; Yang, J.; Lei, Y.; Cao, F. *Chem. Mater.* **2007**, *20*, 198.
(37) Jia, B.; Gao, L. *J. Phys. Chem. C* **2008**, *112*, 666.

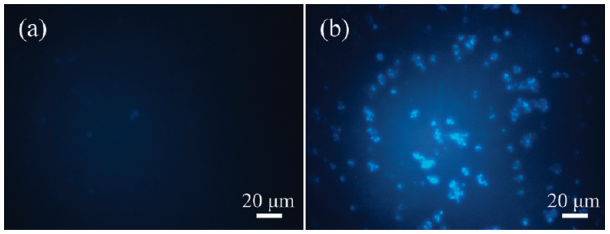

Figure 6. Fluorescence microscopy images of (a) Fe_3O_4 and (b) Fe_3O_4@ZnS microspheres.

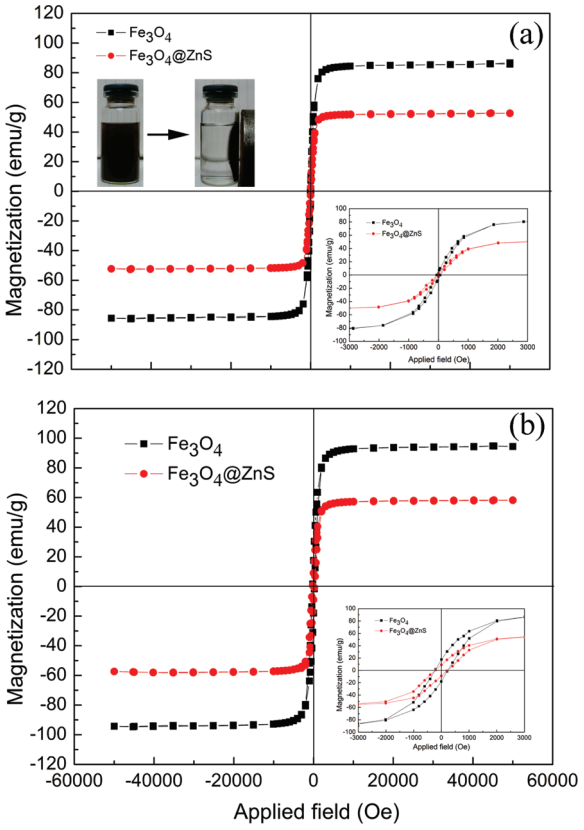

Figure 7. Magnetic hysteresis loops of as-synthesized Fe_3O_4 microspheres and Fe_3O_4@ZnS microspheres measured at (a) 300 and (b) 5 K. The insets are the magnetic responsive images of Fe_3O_4@ZnS microspheres and the magnified magnetic hysteresis loops, respectively.

have coercive force values of 50.2 Oe (at 300 K) and 223.2 Oe (at 5 K), respectively, which further confirm the typical ferromagnetism of the core−shell spheres.

Figure 8a and 8b are the photographs of Fe_3O_4@ZnS core−shell microspheres before and after UV light irritation when they are subjected to an external magnetic field. The images show that the core−shell spheres can self-assemble and align into simple linear chains structures, which reveal high magnetic sensitivity and manipulability under an external magnetic field. Moreover, the linear chains with strong blue light are observed after using UV light irritation. The combined magnetic-optical properties endow the composites with a promising application in biomedical fields including drug targeting, biomaterials separation, and diagnostic analysis.

3.3. Formation Mechanism of Bifunctional Magnetic-Optical ZnS@Fe_3O_4 Core−Shell Microspheres. On the basis of the above discussion, bifunctional magnetic-optical Fe_3O_4@ZnS core−shell microspheres have been successfully synthesized. To rationally construct and synthesize magnetic-optical composites, it is essential to discuss the reaction details and understand the formation mechanism. The proposed formation mechanism of bifunctional magnetic-optical Fe_3O_4@ZnS core−shell microspheres is depicted in Figure 9.

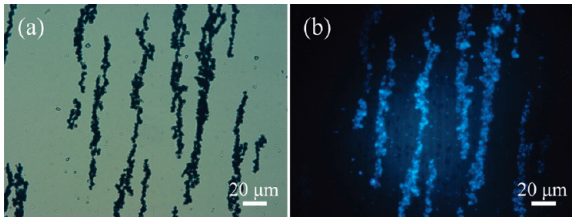

Figure 8. Photographs of the orientation and alignment of Fe_3O_4@ZnS core−shell microspheres under an external magnetic field. (a) Before and (b) after UV light irritation.

There are three distinct stages during the deposition process of ZnS on the surface of Fe_3O_4. Firstly, the hydrophilic groups (SO_4^-) of SDS interact with the surface of Fe_3O_4 microspheres, which can be proved by the FTIR spectra of as-synthesized Fe_3O_4 microspheres (Figure 10a) and Fe_3O_4−SDS microspheres (Figure 10b). The absorption bands around 3448.47 and 1637.44 cm^{-1} correspond to the bending vibration of absorbed molecular water. The strong band at 586.31 cm^{-1} is consistent with the characteristic absorption of Fe_3O_4. Compared with curve a, the relative intensity of the asymmetrical and symmetrical stretching of $-CH_2-$ presenting at 2918.08 and 2850.58 cm^{-1} in curve b increased significantly. The characteristic bands of SO_4^{2-} at 1209.28 cm^{-1} and the symmetrical stretching vibration of S=O at 1080.05 cm^{-1} appeared respectively, which indicate the hydrophilic group (SO_4^-) of SDS interact with the surface of Fe_3O_4 microspheres. After grafting active groups, the Fe_3O_4 microspheres are negatively charged. In addition to the role above mentioned, SDS, as a surfactant, could also prevent Fe_3O_4 microspheres from the aggregation, which caused by magnetic attraction. Second, when $Zn(Ac)_2$ is added into the SDS treated magnetite particles dispersion, the released Zn^{2+} ions would be absorbed on the surface of Fe_3O_4 due to the electrostatic interaction. Finally, the released S^{2-} ions from TAA react in situ with Zn^{2+} ions on the surface of Fe_3O_4 microspheres due to the electrostatic interaction. In this stage, amorphous ZnS was firstly generated on Fe_3O_4 cores at the lower temperature. With increasing reaction temperature, the crystallized ZnS nanoparticles would form and deposit on the amorphous ZnS layer. In the whole reaction process, S^{2-} ions are slowly released from TAA, which plays a key role in formation of uniform ZnS shell on the surface of Fe_3O_4. The slow released rate of S^{2-} ions is in favor of the heterogeneous nucleation of ZnS instead of rapid homogeneous nucleation in the solution.[29]

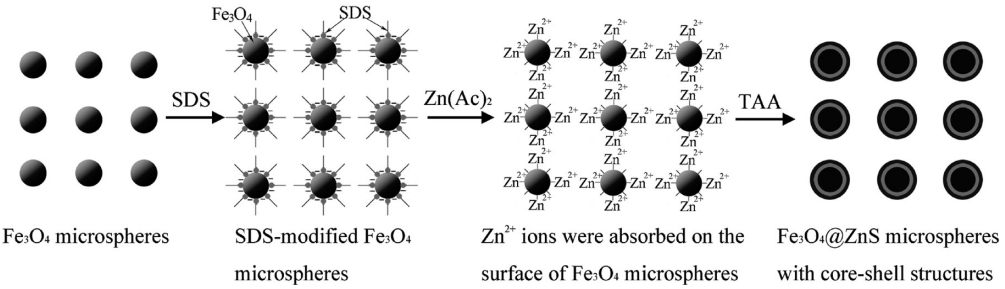

Figure 9. Schematic illustration of the formation mechanism of bifunctional magnetic-optical Fe_3O_4@ZnS core−shell microspheres.

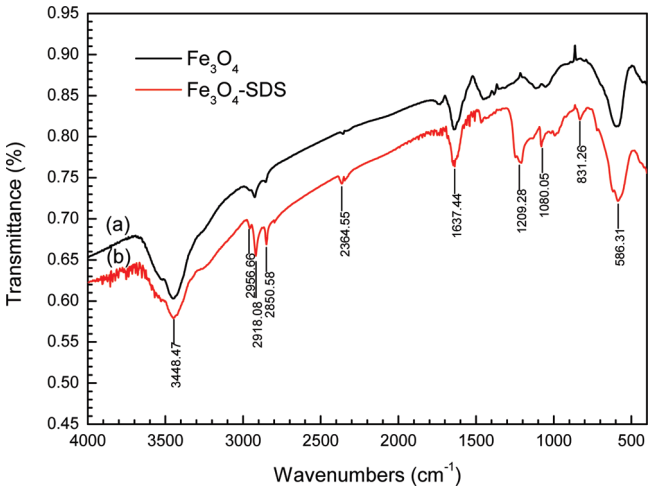

Figure 10. FTIR spectra of (a) as-synthesized Fe_3O_4 microspheres and (b) Fe_3O_4−SDS microspheres.

4. Conclusions

In summary, the present work demonstrates a facile approach to fabrication of bifunctional magnetic-optical Fe_3O_4@ZnS core−shell microspheres by using an anion surfactant. In addition to playing a role in stabilizing, SDS also provides an abundance of active SO_4^- grafting groups, which allow the surface of Fe_3O_4 microspheres negatively charged. Besides, the slow heterogeneous nucleation process of ZnS plays a key role in the reaction because of the lower released rate of S^{2-} ions hydrolyzed from TAA. The presented core−shell composites offer two distinct functionalities: (1) the inner Fe_3O_4 cores imbue the composites with robust magnetic responsive properties and manipulability, (2) the outer ZnS shells have strong fluorescent property. Therefore, the obtained bifunctional magnetic-optical Fe_3O_4@ZnS core−shell microspheres have great potential applications in drug targeting, bioseparation, and diagnostic analysis. Furthermore, this facile synthetic procedure may be widely applicable in synthesizing bi- or multifunctional composites with core−shell heterostructures by using different cation or anion surfactants.

Acknowledgment. The authors thank Dr. Guicun Li for his helpful discussion. This research was financially supported by the National Natural Science Foundation of China (NSFC 50672039).

Supporting Information Available: High-magnification TEM image and the corresponding EDS elemental mappings, SEM images, and PL emission spectra of Fe_3O_4@ZnS microspheres with different thickness of ZnS layer, the amounts of the starting materials, and the statistical data of the samples, typical histograms of the particle size, and size distribution (PDF). This material is available free of charge via the Internet at http://pubs.acs.org.